

UNCLASSIFIED

AD NUMBER	
AD019311	
CLASSIFICATION CHANGES	
TO:	unclassified
FROM:	restricted
LIMITATION CHANGES	
TO:	Approved for public release, distribution unlimited
FROM:	Distribution authorized to U.S. Gov't. agencies and their contractors; Administrative/Operational Use; DEC 1952. Other requests shall be referred to Air Force Cambridge Research Laboratories, Hanscom AFB, MA.
AUTHORITY	
AFCRC ltr dtd 21 Jan 1954; AFCRC ltr dtd 28 Oct 1969	

THIS PAGE IS UNCLASSIFIED

Armed Services Technical Information Agency

AD

19311

NOTICE: WHEN GOVERNMENT OR OTHER DRAWINGS, SPECIFICATIONS OR OTHER DATA ARE USED FOR ANY PURPOSE OTHER THAN IN CONNECTION WITH A DEFINITELY RELATED GOVERNMENT PROCUREMENT OPERATION, THE U. S. GOVERNMENT THEREBY INCURS NO RESPONSIBILITY, NOR ANY OBLIGATION WHATSOEVER; AND THE FACT THAT THE GOVERNMENT MAY HAVE FORMULATED, FURNISHED, OR IN ANY WAY SUPPLIED THE SAID DRAWINGS, SPECIFICATIONS, OR OTHER DATA IS NOT TO BE REGARDED BY ANY PERSON OR CORPORATION, OR CONVEYING ANY RIGHTS OR PERMISSION TO MANUFACTURE OR SELL ANY PATENTED INVENTION THAT MAY IN ANY WAY BE RELATED THERETO.

Reproduced by
DOCUMENT SERVICE CENTER
KNOTT BUILDING, DAYTON, 2, OHIO

The following ESPIONAGE NOTICE can be disregarded unless this document is plainly marked RESTRICTED, CONFIDENTIAL, or SECRET.

NOTICE: THIS DOCUMENT CONTAINS INFORMATION AFFECTING THE NATIONAL DEFENSE OF THE UNITED STATES WITHIN THE MEANING OF THE ESPIONAGE LAWS, TITLE 18, U.S.C., SECTIONS 793 and 794. THE TRANSMISSION OR THE REVELATION OF ITS CONTENTS IN ANY MANNER TO AN UNAUTHORIZED PERSON IS PROHIBITED BY LAW.

19311
19312
19313
19314
AD 110-19312
AD 110-19313
AD 110-19314
SECURITY INFORMATION

RESTRICTED

AIR FORCE SURVEYS IN GEOPHYSICS

No.23

WEATHER EFFECTS ON RADAR

D. ATLAS

J. S. MARSHALL

V. G. PLANK

T. W. R. EAST

W. H. PAULSEN

K. L. S. GUNN

A. C. CHMELA

W. HITSCHFELD

DECEMBER 1952

GEOPHYSICS RESEARCH DIRECTORATE

AIR FORCE CAMBRIDGE RESEARCH CENTER

AIR RESEARCH AND DEVELOPMENT COMMAND

RESTRICTED

THE EFFECTS OF WEATHER ON RADAR

PART I THE MICROWAVE PROPERTIES OF PRECIPITATION PARTICLES*

By J. S. Marshall, T. W. R. East, and K. L. S. Gunn

McGill University, Montreal

PART II ATMOSPHERIC ATTENUATION OF THE SHORT MICROWAVES

By David Atlas, V. G. Plank, W. H. Paulsen, and A. C. Chmela

Air Force Cambridge Research Center

APPENDIX A OXYGEN ABSORPTION

By David Atlas

Air Force Cambridge Research Center

APPENDIX B CALCULATED SENSITIVITY OF AIRBORNE WEATHER RADARS

By J. S. Marshall and Walter Hitschfeld

McGill University

*The research reported in Part I has been sponsored by the Geophysics Research Directorate of Air Force Cambridge Research Center, Air Research and Development Command, under Contract No. AF19(122)-217.

SECURITY INFORMATION RESTRICTED

PREFACE

In recent years, the trend of airborne radars has been toward shorter and shorter wavelengths where the atmosphere becomes increasingly more opaque and weather clutter becomes increasingly more frequent and intense. Since either or both of these factors may seriously limit the use of such short wavelengths, an assessment of their magnitudes is of considerable importance. A comprehensive evaluation of this sort was made by Ryde (1946) whose work remains as the one outstanding authoritative reference in this field.

Ryde concerned himself with the extremely broad problem related to the detection of targets in and through clouds and precipitation. His interest included the wavelength region from 1 - 10 cm, with emphasis on the upper end of this band. Among other things, he considered the basic scattering and absorption cross-sections of the various atmospheric constituents and applied these to the computation of the magnitude of the echo intensity and attenuation due to each component individually. Although Ryde's work is applicable almost in its entirety today, the results of more recent research should be added, and minor modifications made. In addition, detailed consideration should be given to the wavelengths shorter than 3 cm, the region which is just now being fully exploited. Finally, it is of some practical interest to evaluate the cumulative effects on the atmosphere's transparency of the various atmospheric constituents in the amounts and combinations which are likely to be found under typical or extreme weather conditions. These are, in essence, the objectives of this report.

In Part I, Marshall, East, and Gunn have made a fairly comprehensive survey of the state of knowledge of scattering and attenuation by the atmosphere. This includes some previously unpublished and important work by Haddock (1948). It contains in direct or indirect form the answers to most of the solvable problems which have been, or may be raised in this general field. However, an all-inclusive study would require practically a complete repetition of Ryde's excellent 1946 paper. Because of the comprehensive nature of the latter paper, it is recommended that this report be used in conjunction with it. Wherever the present work supersedes Ryde's paper, by virtue of the use of more recently determined constants or theoretical information, it will be specifically mentioned.

Perhaps a statistical study as that made by Bussey (1950) would be of some practical utility to those interested in the average effects of the atmosphere on microwave transmission. In that study, Bussey computed the frequency with which various attenuation coefficients could be expected to be exceeded in the vicinity of Washington, D.C. The results depend, of course, on the local rainfall and water vapor statistics although they may be extrapolated, with caution, to areas of similar rainfall regimes. The information is restricted, furthermore, to the lower layers of the atmosphere.

The present and potential uses of microwave techniques by the Air Force generally involve transmission through the vertical dimension of the atmosphere. Since the vertical distribution of the several attenuating elements (rain, snow, clouds, oxygen, and water vapor) is generally very complex, and since few statistics are available on the frequencies with which they occur in various combinations, no satisfactory estimate can presently be made of

the amount of time during which losses of certain magnitude can be expected. Instead, in Part II of this report an attempt has been made to select some typical idealized cloud and precipitation conditions and to compute the resultant opacity of the atmosphere in each case. The reader may then select one or more of these models and corresponding losses as typical of the average or extreme conditions under which his radar may be required to operate. Such an approach to the problem may well result in a better estimate of typical losses than a statistical survey which is based on the necessarily crude use of scanty data.

The weather models of Part II are based primarily on physical considerations, and are therefore largely independent of geographical location. The frequency of occurrence of each type of situation may vary widely from place to place, but no attempt has been made to treat such climatological problems. However, the cloud densities and rates of precipitation have been described, by adjective ratings of "high, low, or moderate" corresponding roughly with conditions generally observed in temperate United States.

An Appendix, a report entitled "Calculated Sensitivity of Airborne Weather Radars", became available during the publication process. Acknowledgment is made to J. S. Marshall and Walter Hitschfeld of McGill University for this paper. The original work was performed under joint sponsorship of Aeronautical Radio, Inc., and the Air Transport Association of America. Aeronautical Radio, Inc., has kindly granted permission for reproduction of this paper as an appendix to this report.

The authors are indebted to Mr. Ralph J. Donaldson for valuable criticism and editing.

PART I: THE MICROWAVE PROPERTIES OF PRECIPITATION PARTICLES

	Page
1. INTRODUCTION	1
2. REFRACTIVE INDEX	5
3. SPHERICAL PARTICLES	
3.1 Mie Theory	9
3.2 Small Particles (Rayleigh)	10
3.3 Larger Particles	11
3.4 Water-Coated Ice Particles	15
4. RAIN	
4.1 Drop Size-Distributions	17
4.2 Scattering by Rain	19
4.3 Attenuation by Rain	22
4.4 Shaped Raindrops	26
5. SNOW	
5.1 Scattering by Snow	27
5.2 Attenuation by Snow	28
5.3 Wet Snow and the Bright Band	29
6. CLOUDS	
6.1 Scattering by Clouds	30
6.2 Attenuation by Clouds	31
7. ATMOSPHERE	
7.1 Scattering	32
7.2 Attenuation	33
8. THE DIRECTION OF FUTURE RESEARCH	
8.1 Refractive Indices	39
8.2 Rain	39
8.3 Snow	40
8.4 Cloud	41
8.5 Atmosphere	41

PART II: ATMOSPHERIC ATTENUATION OF THE SHORT MICROWAVES

	Page No.
1. Introduction	1
2. Discussion and Results	2
2.1 Case I: Standard (Maritime Polar) Air; Case II: Maritime Tropical Air	2
2.2 Non-vertical Paths	7
2.3 Case III: An Ice Cloud in Maritime Polar Air Overrunning Modified Continental Polar Air	9
2.4 Case IV: Heavy Snow Falling From a Dense Mixed Water-Ice Cloud in an Atmosphere Otherwise Similar to Case III.	13
2.5 Case V: A Thick Dense Water Cloud in Maritime Polar Air	17
2.6 Case VI: Heavy Snow Turning to Rain and Falling Through Dense Water Cloud	19
2.7 Case VII: Viewing the Ground from above an Intense Thunderstorm in Maritime Tropical Air	23
2.8 Case VIII: Viewing the Ground from behind an Intense Thunderstorm	25
2.9 Approximate Statistical Data	26
3. General Summary	29
3.1 Comparison of Cases	29
3.2 Cumulative Losses versus Height	33
3.3 The Effect of Using the Lower Oxygen Attenuation Coefficient	33
3.4 Optimum Flight Altitude	35
4. Conclusions	37
Appendix A - Oxygen Absorption	40
Appendix B - Calculated Sensitivity of Airborne Weather Radars	

AD No. 19311
ASTIA FILE COPY

PART I

THE MICROWAVE PROPERTIES OF PRECIPITATION PARTICLES

by

J. S. Marshall

T. W. R. East

K. L. S. Gunn

McGill University

Montreal, Canada

1. INTRODUCTION

In the comparatively new subject of radar-meteorology, the theoretical paper by Ryde (1946) stands out. In it he predicted the back-scatter and attenuation by meteorological phenomena, and, in almost every respect, the results obtained in experiments have confirmed the predictions. The present contribution will review the theoretical problem in the light of developments in the years that have elapsed since Ryde's work was done, and with reference to the experimental results.

Meteorological radar equipment provides information about the structure or pattern and about the quantity of precipitation. This paper will not be concerned with the structural information obtained, but will consider the scattering from a small region in which the properties of the precipitation can be taken to be uniform, and the attenuation taken along a path of propagation as a whole.

Plane electromagnetic waves travelling through air containing precipitation are scattered and absorbed by the particles of ice, snow or water. Ice particles scatter some of the radiation in all directions, but in most cases of interest do this conservatively, without converting any into thermal energy, since ice is very nearly a perfect dielectric. Water, with its larger dielectric constant, scatters more strongly than ice; in addition, it has considerable dielectric loss and a large part of the attenuation by rain is due to thermal dissipation.

Three quantities with the dimensions of area are derived for a particle in the path of a plane travelling wave. The back-scatter cross-section σ is defined in such a way that σ multiplied by the incident intensity would be

the total power radiated by an isotropic source which radiates the same power in the backward direction as the scatterer. The "scattering cross-section" Q_s is such that Q_s , multiplied by the incident intensity, is the power scattered by the particle. The "total absorption cross-section" Q_t is such that Q_t times the incident intensity is the total power taken from the incident wave.

The scattering properties of precipitation have made possible extensive use of microwave radar sets for meteorological purposes. The radar signal from precipitation is, however, not steady like that from a point target. The received power at any instant is made up of the resultant of the signals from a very large number of particles, and depends on their exact arrangement in space, which is being continually changed by the turbulent motion of the air. Marshall and Hitschfeld (1952) have shown that an instantaneous observation of received power gives very little information about the precipitation, and the signal at any given range has to be averaged until a large number of independent returns have been received.

This can be arranged by using a long-persistence display or by photographic recording so that the returns from many transmitter pulses are combined.

The equation for the average received power $\overline{P_r}$ is

$$\overline{P_r} = \frac{P_t A_e h}{8\pi r^2} \sum_1 \sigma \quad (1.1)$$

where P_t is the transmitted power,

h is the length of the pulse in space,

r the range from which the signal is being received,

A_e the equivalent antenna aperture,

$\sum_1 \sigma$ the total back-scatter cross-section of the particles in unit volume.

The received power is proportional to h so that the sensitivity of the system can be increased by lengthening the transmitter pulse. (If this change is accompanied by a reduction in receiver bandwidth, a further improvement in signal-to-noise ratio is obtained.) However, the range resolution is correspondingly reduced. Increasing A_e , on the other hand, improves both sensitivity and angular resolution, so that the antenna is made as large as practicable.

The equivalent aperture A_e is less than the actual area of the antenna for two reasons. Firstly, not all the power coming from the primary feed falls inside the parabolic reflector, neither is the distribution of power uniform across the aperture (see e.g. Silver (1949) section 6.4). In normal radar systems the effective aperture A' for a point target is about 65% of the actual aperture. The second reason which applies only to distributed targets affects weather radars. Some of the radiated power goes into side-lobes and the edges of the main beam, and though all of it strikes precipitation, some of the returned power comes from directions to which the antenna is less sensitive for reception. This means that the average receiving aperture A_e for all parts of the target is less than A' , the value for the central portion.

The fact that the target normally fills the beam at any range accounts for the inverse square law for received power versus range, in place of the usual fourth power law for a point target such as an aircraft. Though equation (2.1) does not mention wavelength explicitly, σ increases rapidly as the wavelength decreases, as discussed in the next section.

It will be shown in section 3.2 that for a wavelength λ long compared with the diameter D of the particles, the approximation

$$\sigma = \frac{\pi^5 D^6}{\lambda^4} |K|^2 \quad (1.2)$$

can be used, where $|K|^2$ depends on the dielectric constant of the material and varies only slowly with wavelength (chapter 2). From (1.1) and (1.2) we have

$$\overline{P_r} = \frac{\pi^4 P_t A_g h}{8\pi^2 \lambda^4} \sum_1 D^6 |K|^2. \quad (1.3)$$

So far we have neglected the attenuating effect of any precipitation through which the signal may have to pass.

The intensity of plane parallel radiation in traversing distance x through uniform precipitation is reduced from I_0 to I , where

$$I = I_0 \exp \left\{ -x \sum_1 Q_t \right\}. \quad (1.4)$$

The summation is over all the particles in unit volume. In practical units, the attenuation per kilometre of path length is

$$\text{attenuation (db/km)} = 0.4343 \sum_1 Q_t, \quad (1.5)$$

where the summation is over one cubic metre and Q_t is now in cm^2 . For the case of wavelength long compared to the drop diameters (section 3.2), we can use an approximation for Q_t , equation (3.7), so that equation (1.5) becomes

$$\text{attenuation (db/km)} = 0.4343 \frac{\pi^2}{\lambda} \sum_1 D^3 \text{Im}(-K). \quad (1.6)$$

For radar, the radiation travels there and back, so the numerical constant should be doubled to obtain decibels per kilometre of range.

The exact equation for the average received power \overline{P}_r is, then

$$\begin{aligned}\overline{P}_r &= 10^{-0.8686 \times \frac{Q_1}{1}} \cdot \frac{P_t A_r h}{4\pi r^2} \frac{Q_1}{1} \\ &= 10^{-0.8686 \times \frac{Q_1}{1}} \cdot \frac{\pi^2}{8} \frac{P_t A_r h}{r^2 \lambda} \frac{Q_1}{1} |K|^2,\end{aligned}$$

where the Rayleigh approximation is applicable.

If the attenuation of the precipitation is not uniform along the path, the factor $\times \frac{Q_1}{1}$ must be replaced by $\int \frac{Q_1}{1} dx$ over the path.

2. REFRACTIVE INDEX

To calculate the scattering and attenuation of electromagnetic waves by particles in the atmosphere, one must know the values of the complex dielectric constant ϵ for the temperature and wavelength under consideration.

The square root of the dielectric constant n may be written

$$n = n - i\kappa,$$

where n is the refractive index and κ the absorption coefficient of the material. In general, the scattering and attenuation are complicated functions of n (chapter 3), but in the special case of wavelength long compared to diameter,

$$\text{back-scatter} \propto |K|^2 \quad (1.3)$$

$$\text{attenuation} \propto \text{Im}(-K) \quad (1.6)$$

$$\text{where } K = \frac{n^2 - 1}{n^2 + 2}.$$

For a given substance n is a function of wavelength and temperature. Saxton (1946) measured values of n and k for water at a few wavelengths and calculated other values in the centimetric band, for temperatures from 0° to 40°C . Recently Lane and Saxton (1952) have reported additional measurements at a lower wavelength (6.2 mm) and some more accurately determined values at 1.24 and 3.2 cm. As well, they have determined values of k for supercooled water down to -6°C at three wavelengths (see section 4.3).

In table 2.1, the variation of the refractive index with temperature and wavelength is shown, and the quantities $\text{Im}(-K)$ and K^2 have been calculated. Values for n and K are taken from Kerr (1951) for 10 cm wavelength, and directly from Lane and Saxton (1952) for the other wavelengths.

Measurements of the quantities n and k for ice show that in the centimeter band both n and K are practically independent of λ . Dunsmuir and Lamb (1945) and Lamb (1946) found k to be a very small quantity, ranging from 1.2×10^{-3} at 0°C , through 1.9×10^{-4} at -20°C to 1.3×10^{-4} at -40°C . More recent measurements by Cumming (1952) give values for k roughly twice those of Lamb; Cumming's value at -12°C agrees with one obtained at that temperature by the MIT Dielectric Laboratory (Cumming 1952). Both Cumming and Lamb and Turney (1949) agree on a value of $n = 1.78$ for ice, constant over the temperature range 0 to -20°C . The refractive index data for ice is summarized in Table 2.2.

Snow may be considered as a mixture of two dielectrics, ice and air. According to Debye (1929), one can calculate the ratio $\frac{K}{\rho}$ for a mixture of two dielectrics by adding the $\frac{K}{\rho}$ values for the two substances in proportion

Table 2.1

Variation of Refractive Index of WATER with Temperature and Wavelength

$T^{\circ}\text{C}$ / λ cm	10	3.21	1.24	0.62	
n	20	8.88	8.14	6.15	4.44
	10	9.02	7.80	5.45	3.94
	0	8.99	7.14	4.75	3.45
	-8		6.48	4.15	3.10
k	20	0.63	2.00	2.86	2.59
	10	0.90	2.44	2.90	2.37
	0	1.47	2.89	2.77	2.04
				2.55	1.77
$ k ^2$	20	.928	.9275	.9193	.8926
	10	.9313	.9282	.9152	.8726
	0	.9340	.9300	.9055	.8312
	-8			.8902	.7921
$\text{Im}(-k)$	20	.00474	.01883	.0471	.0915
	10	.00688	.0247	.0615	.1142
	0	.01102	.0335	.0807	.1441
	-8			.1036	.1713

to the mass of each. Neglecting the contribution of $\frac{K}{\rho}$ for air, then $\frac{K}{\rho}$ for ice of any density is practically constant. Cumming (1952) made measurements of the dielectric constant of snow of various densities. Using his data one finds that $\frac{K}{\rho}$ varies more or less uniformly from 0.46 for ice of density 0.917 gm cm^{-3} to 0.50 for density 0.22 gm cm^{-3} .

Table 2.2

Variation of Refractive Index of ICE with Temperature
(based on data from Cumming, 1952)

n		1.78	At all temperatures
k	0C	2.4×10^{-3}	
	-10	7.9×10^{-4}	
	-20	5.5×10^{-4}	
$ k ^2$		0.197	At all temperatures. This is for ice of unit density, the value to be used when D is diameter of melted ice particle, in equation (1.3) Marshall and Gunn (1952) .
$\text{Im}(-k)$	0C	9.6×10^{-4}	
	-10	3.2×10^{-4}	
	-20	2.2×10^{-4}	

3. SPHERICAL PARTICLES

3.1 Mie's Theory

A complete theory for spherical particles of any material in a non-absorbing medium was developed by Gustav Mie (1908). Mie's work has been restated by Stratton (1941), Goldstein (1946) and by Kerr (1951). Using the notation of these later workers, the cross-sections of a spherical particle are

$$\sigma = \frac{\lambda^2}{4\pi} \left| \sum_{n=1}^{\infty} (-1)^n (2n+1) (a_n - b_n) \right|^2 \quad (3.1)$$

$$Q_s = \frac{\lambda^2}{2\pi} \sum_{n=1}^{\infty} (2n+1) (|a_n|^2 + |b_n|^2) \quad (3.2)$$

$$\text{and} \quad Q_t = \frac{\lambda^2}{2\pi} (-\text{Re}) \sum_{n=1}^{\infty} (2n+1) (a_n + b_n) \quad (3.3)$$

where λ = wavelength in the medium,

a_n = coefficient of the n th magnetic mode,

b_n = coefficient of the n th electric mode.

The coefficients a_n and b_n are given in Appendix II in terms of Spherical Bessel Functions of order n . The arguments of the functions are α and m and contain the properties of the sphere and the wavelength. The quantity $\alpha = \frac{\pi D}{\lambda}$, where D is the diameter of the sphere. The quantity m is the complex refractive index of the material relative to the medium, and $m = n - jk$, where n is the refractive index, and k , the absorptive index.

Equations (3.2) and (3.3) have been computed by Lowan (1949) for water spheres at 18°C for various wavelengths between 3 μ m and 10 μ m.

3.2 Small Particles (Rayleigh Approximation)

By expanding the a 's and b 's in ascending order of α for $n = 1, 2, \dots$, formulae for Q_e and Q_m can be obtained which apply to small values of α . Neglecting terms of higher than sixth power of α , only a_1 , b_1 and b_2 are significant, and they are

$$a_1 = -\frac{1}{45} (n^2-1) \alpha^5 \quad (3.4a)$$

$$b_1 = -\frac{21}{3} \frac{n^2-1}{n^2+2} \alpha^3 \left(1 + \frac{3}{5} \frac{n^2-2}{n^2+2} \alpha^2 - \frac{21}{3} \frac{n^2-1}{n^2+2} \alpha^3 \right) \quad (3.4b)$$

$$b_2 = \frac{1}{15} \frac{n^2-1}{2n^2+3} \alpha^5. \quad (3.4c)$$

For diameters small compared with the wavelength, we can obtain approximate formulae for σ and Q_e by putting $\alpha \ll 1$ into these equations. Then, only the leading term of b_1 , the coefficient of the first electric mode, need be considered, and the contribution to σ and Q_e of all higher order terms in the a 's and b 's can be neglected. The resulting formulae are known as the Rayleigh approximations:

$$\sigma = \frac{\lambda^2}{2\pi} \cdot 2 \alpha^6 \left| \frac{n^2-1}{n^2+2} \right|^2 = \frac{\pi^5 |k|^2}{\lambda^4} D^6 \quad (3.5)$$

$$Q_e = \frac{\lambda^2}{2\pi} \cdot \frac{4}{3} \alpha^6 \left| \frac{n^2-1}{n^2+2} \right|^2. \quad (3.6)$$

The total absorption cross-section Q_t is given by equation (3.3) in which the real parts of the coefficients a and b have to be obtained. In this case, however, it does not always happen that the leading term in b_1 contributes the most to Q_t . Indeed, if n is purely real, the α^3 and α^5 terms of b_1 are imaginary and contribute nothing to Q_t , and of the terms listed in equation (3.4) only the α^6 term of b_1 will appear in Q_t .

At this stage it is convenient to introduce a fourth cross-section Q_a , the absorption cross-section, to account for the power taken from the incident wave which is dissipated internally as heat and not scattered; it is simply $Q_t - Q_s$. Putting $\alpha \ll 1$ the contribution to Q_t of the α^6 term in b_1 , is the same as the leading term in Q_s , so that this term does not appear in Q_a . Then the leading term in Q_s is given by (3.6) and the leading term in Q_a comes from the α^3 term in b_1 and is given by

$$Q_a = \frac{\lambda^2}{2\pi} \cdot 2 \alpha^3 \operatorname{Im} \left(-\frac{n^2-1}{n^2+2} \right) \quad (3.7)$$

and, of course,

$$Q_t = Q_a + Q_s. \quad (3.8)$$

For a pure lossless dielectric $Q_a = 0$ so that $Q_t = Q_s$ and is given by (3.6). For a very lossy dielectric like water and particle sizes such that $\alpha \ll 1$, $Q_s \ll Q_a$ (figure 3.2) so that $Q_t = Q_a$ and is given by (3.7). For ice at OC and in the size range of snowflakes, at centimetre wavelengths Q_s and Q_a are comparable and both must be calculated; Q_t is their sum.

3.3 Larger Particles

F. T. Haddock (1948) has computed for water at 18°C the ratio between Q_t , calculated from Lowan's (1949) Bureau of Standards tables, and Q_t , calculated from equation (3.7). This ratio $Q_t(\text{Mie})/Q_t(\text{Rayleigh})$ is plotted in figure 3.1 for various wavelengths. Ryde's (1946) figure 3 is a similar plot, but of

$$f_a = \frac{Q_t(\text{Mie})}{\text{geometrical cross-section}}$$

for a wavelength a little over 1 cm.

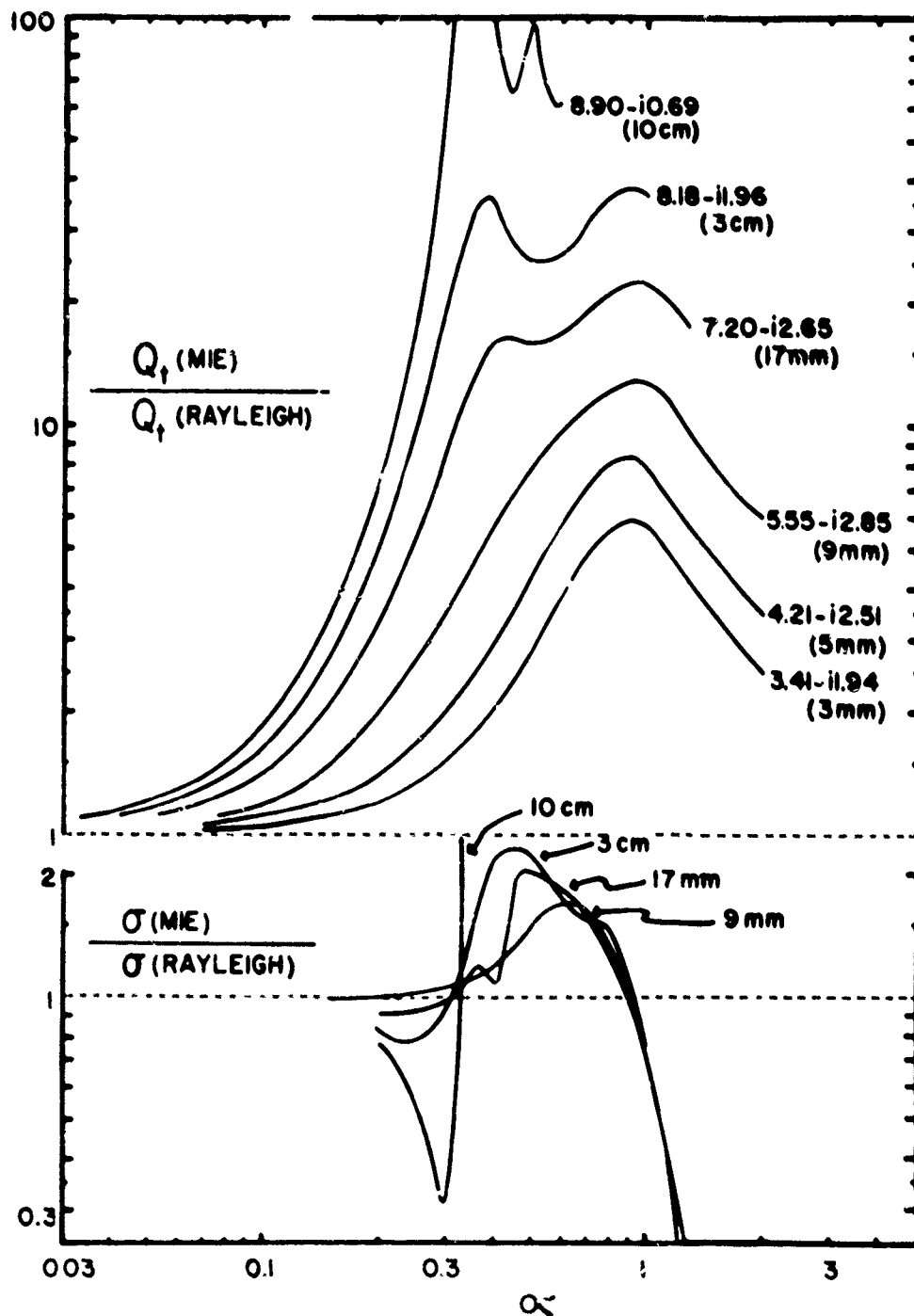


FIG. 3.1 - Ratio of actual attenuation (upper) and actual back-scattering (lower) to that given by the Rayleigh approximation, for water at 38°C.

We can interpret these curves a little further by examining the relative magnitudes of the terms in equation (3.1). For example, for water at 18°C, and $\lambda = 3.0$ cm, we find that the parts of the a's and b's affecting Q_e are

$$\text{Re } [a_1] = -0.209 \alpha^5$$

$$\text{Re } [b_1] = (0.0121 \alpha^3 + 0.0160 \alpha^5) + 0.411 \alpha^6$$

$$\text{Re } [b_2] = -0.000515 \alpha^5$$

up to α^6 .

As long as $\text{Re } [b_1]$ is much greater than $\text{Re } [a_1]$, only the α^3 term is important, but at $\alpha = 0.131$, $\text{Re } [a_1] = \text{Re } [b_1]$, so that Q_e is about twice the Rayleigh value. As α increases beyond this, Q_e tends to an α^5 law, until other terms become more important.

The region of α in which the exact value of Q_e given by (3.3) and the approximate value given by equation (3.8) [i.e. by (3.6) + (3.7)] are nearly equal is known as the "Rayleigh region for attenuation". The diameters of cloud particles are well inside this region for all wavelengths down to 3 mm. This will be discussed in section 4.

The corresponding situation for back-scatter is shown also in figure 3.1. Here $\sigma(\text{Mie})/\sigma(\text{Rayleigh})$ is plotted against α for various wavelengths. We shall define the "Rayleigh region for back-scatter" as the region for which this ratio lies between $\frac{1}{2}$ and 2. It will be seen that for wavelengths up to 17 mm, the ratio stays within these limits up to about $\alpha = 1$, where it falls rapidly. However, at longer wavelengths the ratio first rises beyond 2 so that the region only extends to $\alpha = 0.4$ or less.

At 17 mm wavelength, the Rayleigh region as defined here extends to 6 mm diameter and includes all normal raindrop sizes. At shorter wavelengths, the limit occurs at smaller diameters, so that at $\lambda = 3$ mm, only particles less than 1 mm diameter are inside it. At 3 cm wavelength, the region is also reduced, extending only to 3 mm diameter, but at $\lambda = 10$ cm it covers all raindrop sizes so that the approximate formula can be safely used on rain.

The ratio Q_s/Q_t for water at 15°C, that is the proportion of the total absorption cross-section which is due to scattering, has been computed from Lowan's (1949) tables. This is presented in figure 3.2 for values of α up to 5 (i.e. covering a range of diameter up to 0.6 cm and wavelengths from 3 mm to 10 cm). It will be seen that the curves very roughly coincide, so that for diameters and wavelengths where $\alpha = 0.8$ this fraction is 50%, and where $\alpha = 0.5$ the fraction is 25%. There seems to be no obvious physical reason for this result.

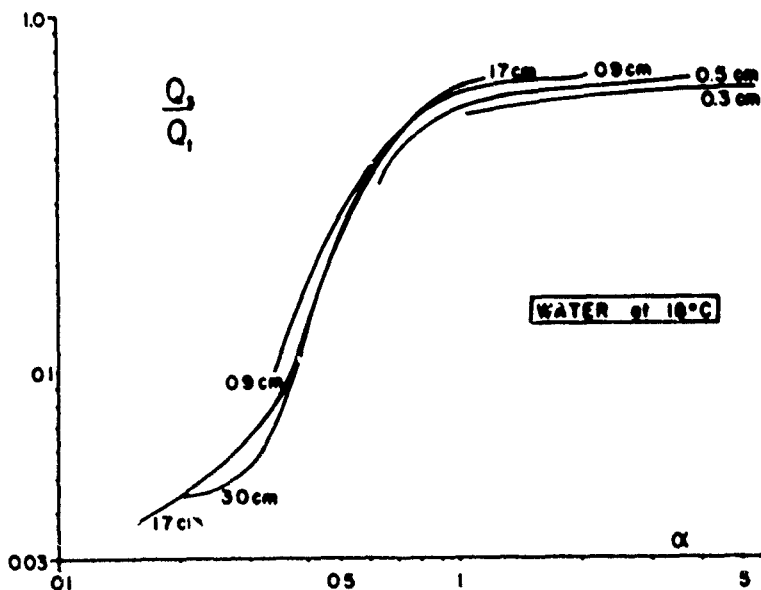


FIG. 3.2 - Ratio of scattering to total cross-sections for water spheres.

3.4 Water-Coat & Ice Spheres

Aden and Kerker (1951) extended Mie's theory to concentric spheres.

^{*}
Langleben and Gunn (1952) have applied this extended theory to spheres of ice coated with water in the region $\alpha \leq 1$. They consider a sphere which changes gradually from all ice to ice coated with water, and finally to all water, maintaining constant mass. The calculated cross-sections for such a particle are plotted against the ratio of the mass of water to total mass in figure 3.3 for 3 cm wavelength and 1.2 mm diameter initially. As the thickness of the water coating increases from zero, the quantities σ , Q_s and Q_t all increase rapidly from their values for ice; when the sphere is still 70% ice (so that the water thickness is less than one-tenth of the total radius)

σ and Q_s are already nearly equal to those for the all-water sphere.

Earlier still, Q_t reaches a maximum value, about twice as great as that for water. No simple explanation can be offered as yet for this extremely rapid increase of the attenuation to twice the all-water value. For other wavelengths and diameters in the Rayleigh region, the curves for Q_s , σ and Q_t are very similar to those of figure 3.3. For larger values of α , the scattering cross-sections do not rise so early, and Q_t does not show such an extreme behaviour.

^{*} Langleben, M. P. and K. L. S. Gunn, 1952: Scattering and absorption of microwaves by a melting ice sphere. Stormy Weather Research Group, McGill University, Scientific Report MW-5, under USAF Contract AF 19(122)-217.

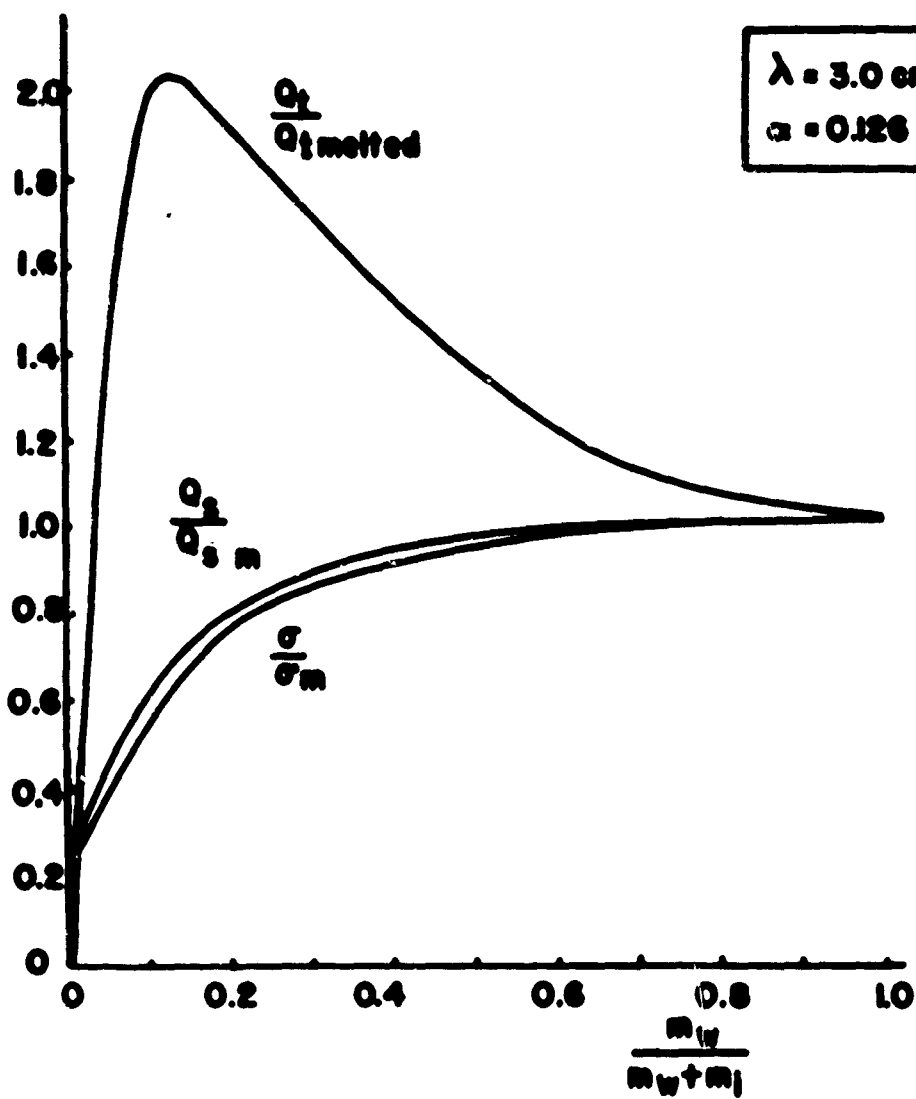


FIG. 3.3 - Relative cross-sections of water-coated ice spheres.

4. Rain

4.1 Drop Size-Distributions

Where Rayleigh theory is applicable, radar can be used to measure the quantity $\sum_1 D^6$. A more significant quantity meteorologically is the rainfall rate, $R = \frac{\pi}{6} \rho \sum_1 v_D D^3$ (where v_D is the terminal velocity of a drop of diameter D). To relate the two quantities the drop size-distribution must be observed. Distributions for rain at the ground have been determined in various parts of the world, and the distribution law, the water content M , the rainfall rate R , and the radar quantity Z can all be related empirically.

(For example, see Wexler (1948), Marshall and Palmer (1948), Hood (1950) etc.)

Various workers have calculated simultaneous values of Z and R from the distribution of drop sizes obtained on a horizontal surface (e.g. Marshall, Langille and Palmer, 1947). Then from a number of such simultaneous values plotted on log-log paper a locus of best fit for the data of the form $Z = aR^b$ can be computed. There have been many such Z/R relations quoted in the literature in the past ten years, which give a wide range of Z values for a given R . Out of these, the authors have found eight relations which are based on measurements using raw drop size-distribution data. These, along with pertinent information, are included in Table 4.1.

The number of points used to make up the different loci varies from worker to worker, as does the range of rainfall rates covered. The great majority of the points in each case lie between 5 and 50 mm hr⁻¹.

A locus

$$Z = 243 R^{1.57} \pm \text{a factor } 1.22 \quad (4.1)$$

TABLE 4.1

Z	Author	Location	How locus determined
208 R ^{1.53}	Wexler (1948) on Anderson's (1947) data	Hawaii	least squares fit (49 points)
269 R ^{1.55}	Mt. Washington [*] observation (1951)	Cambridge, Mass	least squares fit (63 points)
214 R ^{1.58}	Wexler (1948) on Laws and Parsons' data		least squares fit (98 points)
200 R ^{1.6}	Revised from Marshall and Palmer (1948)	Ottawa	best fit by eye (with a check to centre locus amongst data at that slope) (250 points)
295 R ^{1.61}	Hood (1950)	Ottawa	best fit by eye (270 points)
505 R ^{1.44}	Best (1950)	Shoeburyness	
257 R ^{1.45}	Best (1950)	Inyslas	
436 R ^{1.64}	Best (1950)	East Hill	

will define a band taking in the first five relations. If we include Best's data, the locus becomes ($Z = 364 R^{1.55} \pm$ a factor 1.75). As well, one must recognise that there is a limit on the accuracy with which Z or R can be calculated when samples are taken from relatively small volumes of space. The natural variations due to the methods of sampling usually employed may lead to an uncertainty in Z of as high as $\pm 50\%$. Thus, if one uses a relation such as (4.1), it is probably good to within a factor 2 over a range of moderate rainfalls, say 0.5 to 70 mm/hr. Until more is known about the relationship of the radar quantity Z to a meteorological quantity, such as R , this uncertainty will have to be accepted.

^{*} Mount Washington Observatory, 1951: Contribution to the theory of the constitution of clouds. Quarterly Progress Report of the Mount Washington Observatory staff under USAF Contract no. AF 19(122)-399, Oct. 23.

4.2 Scattering v Rain

The curves in figure 3.1 showed the behaviour of the exact back-scattering cross-sections for single drops. Haddock, in plate 6 of his unpublished report, has evaluated the exact cross-sections for rain of various intensities using the drop size-distribution results of Laws and Parsons (1943). Haddock's data has been replotted in figure 4.1 which shows $\Sigma \sigma_1$ against rainfall for two wavelengths, 3 cm and 0.9 cm. For comparison, the Rayleigh approximate back-scattering cross-sections are shown for these same wavelengths. They are derived from summing equation 3.5 over unit volume and substituting $\Sigma_1 D^6 = 200 R^{1.6}$.

Haddock does not give a plot of the exact $\Sigma \sigma_1$ for wavelengths greater than 3 cm, but the 10 cm curve will be identical to the Rayleigh one at all but the very heaviest rainfalls. At 0.9 cm, the exact back-scattering cross-section is larger than the Rayleigh for low rainfalls; it is the same at a rainfall of about 10 mm/hr and then becomes less quite quickly at higher rainfalls, being some 7.5 db below the Rayleigh value at 10 mm/hr. This rapid divergence of the two functions at 0.9 cm for heavy rainfalls is due to the rapid descent of the Ψ -curve for that wavelength (figure 3.1) at values of α which correspond to raindrop diameters. However, wavelengths shorter than 3 cm are not used in rain because of attenuation. At 3 cm wavelength, the appropriate values of α are somewhat lower, and on the basis of figure 3.1 we should expect the exact cross-section to be above the Rayleigh value for heavy rainfall and below it for light. Haddock's curve in figure 4.1 does not do this, but the difference between either of these "exact" results and the Rayleigh curve does not exceed 2 db in any case.

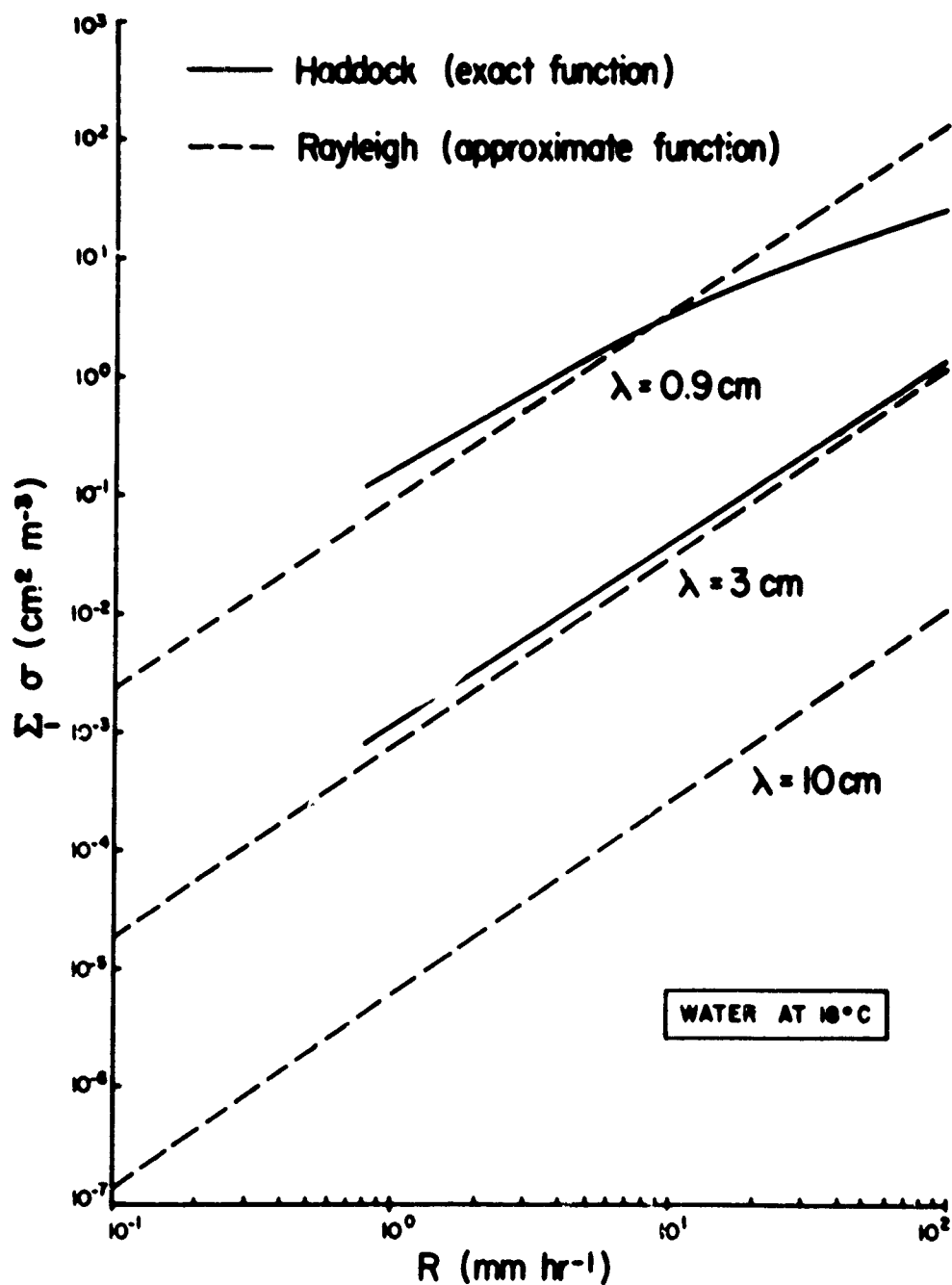


FIG. 4.1 - Exact and Rayleigh approximate back-scattering cross-sections per unit volume of rain-filled space, plotted against rainfall intensity.

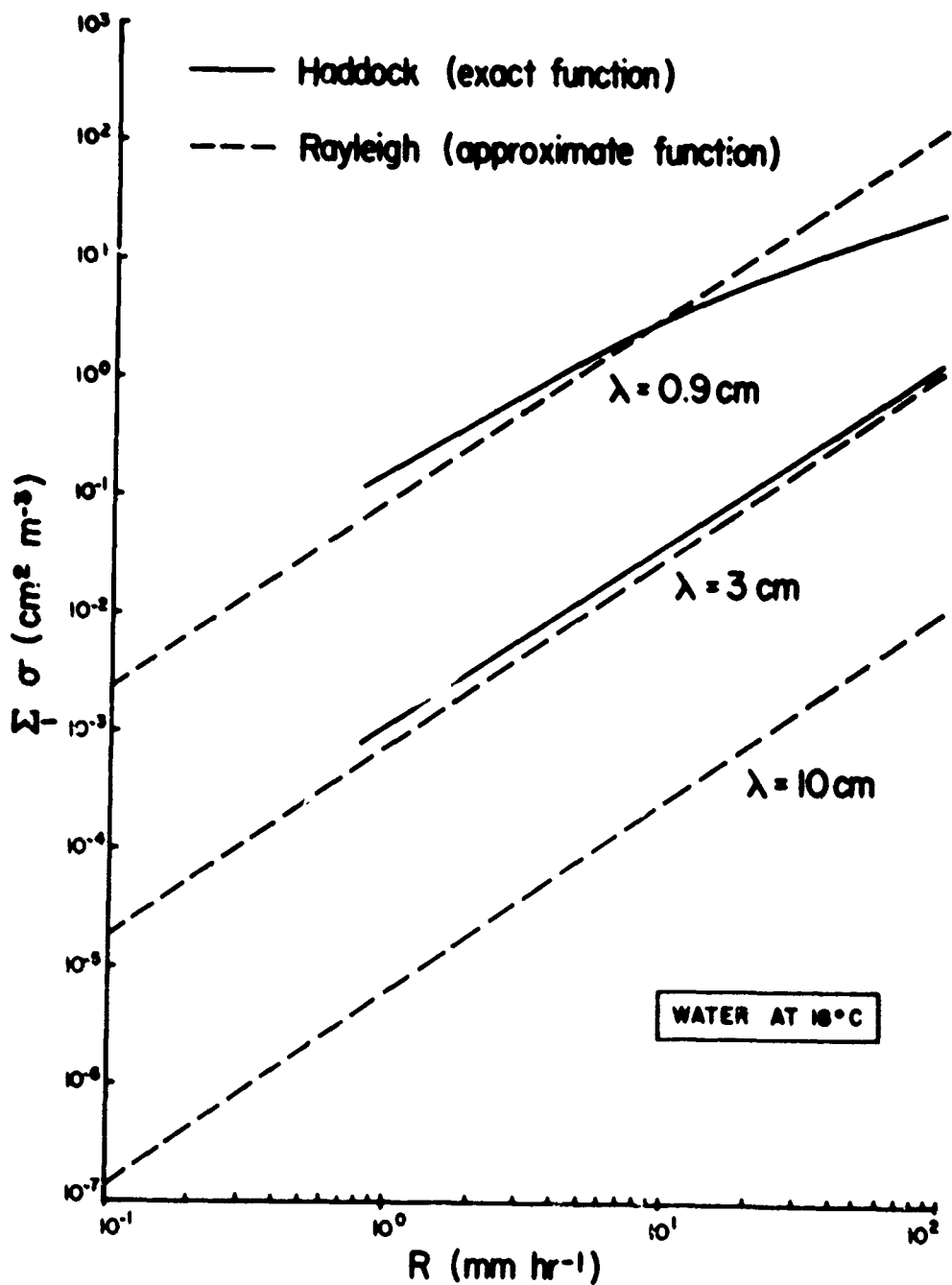
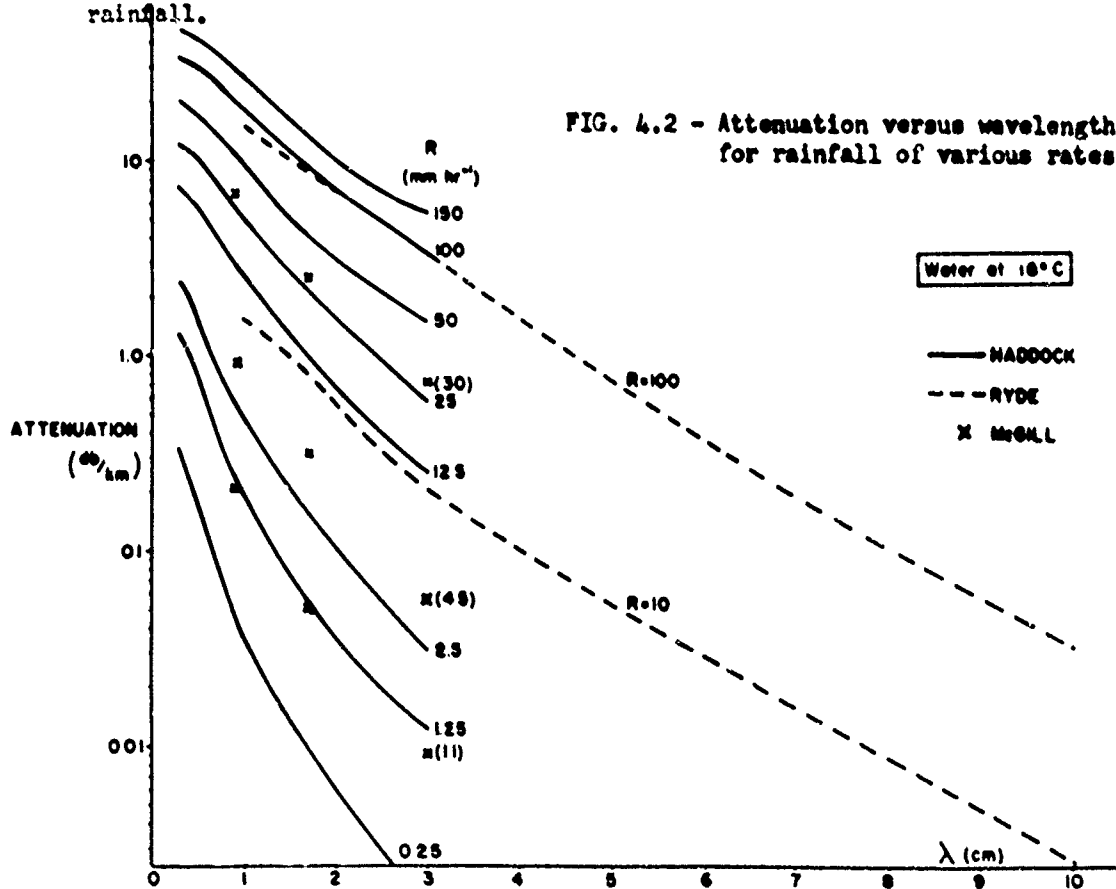


FIG. 4.1 - Exact and Rayleigh approximate back-scattering cross-sections per unit volume of rain-filled space, plotted against rainfall intensity.

4.3 Attenuation by Rain

For rain, the Rayleigh approximation for attenuation does not apply except for wavelengths of 10 cm and longer. Hence the attenuation through rain is not given by equation (1.6), but depends on diameter as well as water content.

The data published by Laws and Parsons has been used by Ryde (1945, 1946) and by Haddock to predict the attenuation at various wavelengths by a given rate of rainfall. The authors have repeated some of Haddock's calculations, using Laws and Parsons' data as plotted by Rigby and Marshall (1952) and Haddock's ratio in figure 3.1. In figure 4.2 these various calculated attenuations are plotted against wavelength for several rates of rainfall.



Some of the same results are replotted in figure 4.3. Here the abscissa is rainfall rate in mm/hr and the ordinate is attenuation divided by rainfall rate. The values given by the Rayleigh approximation (equation 1.6) are shown as broken lines for comparison. The ordinate in this diagram is the factor k in Ryde's (1946) section 7; he suggests that, for many purposes, it may be taken as constant for a given wavelength. At 10 cm wavelength, data is scarce because Lowan's tables cannot be used, but Ryde's two points, together with the knowledge that the Rayleigh value can be used at low rainfall rates, show

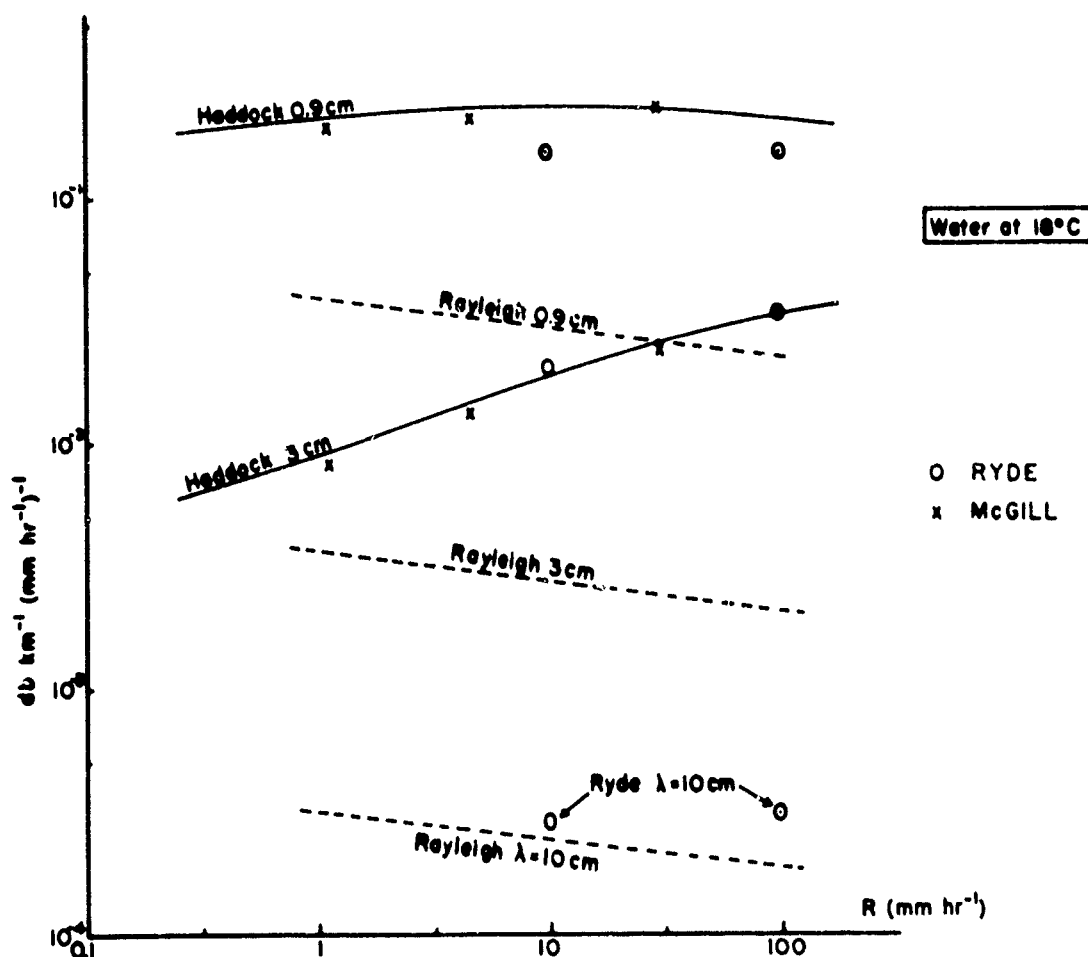


FIG. 4.3 - Attenuation/rainfall versus rainfall for various wavelengths.

that k is very nearly constant, but has such a small value that it is negligible for radar purposes. At 3 cm, k is by no means constant and can be represented reasonably well by the empirical relation $k = 0.009 R^{0.3}$, where R is the rainfall rate in mm/hr. However, if the rainfall rate is known to lie in a restricted range on any particular occasion, a suitable mean value for k could be used. At 9 mm, k is very nearly constant again, though it is 5 to 10 times the corresponding Rayleigh value. This is because Haddock's ratio is near its maximum for these drop sizes at this wavelength.

Whenever k can be taken as constant, the attenuation in db over the path is simply k times the integral of rainfall rate along the path in km-mm/hr.

The data of figure 4.3 is only plotted at widely-spaced wavelengths, so it is not suitable as it stands as a design chart for selecting a wavelength for a particular purpose. It is found, however, that in figure 4.2, which is a log-linear plot, the Ryde curves are nearly straight lines from 3 cm to 10 cm wavelength. At 10 mm/hr, for example, attenuation is halved for an increase of 1.1 cm. At 100 mm/hr, the curve is not so linear but the average slope is similar.

These facts make it possible to interpolate on figure 4.3 and hence predict the wavelength at which a given total attenuation will be encountered over a given path. In Table 7.1, the data for attenuation by rain for four wavelengths at 18C is summarized.

To determine exactly the effect of temperature on the curve of figures 4.2 and 4.3, it is necessary to have a set of curves of Q_t Mie/ Q_t Rayleigh similar to those of figure 3.1 for the refractive indices of water at the required wavelengths at each temperature.^{*} Ryde apparently computed these

^{*} This involves lengthy computations, yielding a set of tables the size of Lowan's (1949) for each temperature.

from first principles for a number of temperatures, since he quotes values for the attenuation at other than 18C (Ryde 1945). At that time he used the refractive index values quoted by Saxton (1946), some of which differ from the more recent values of Saxton and Lane (1952).

An exact evaluation being too lengthy, the authors obtained approximate values for the attenuation at OC for two rainfall rates at wavelengths of 0.9, 1.24, 1.8 and 3.2 cm, by interpolating amongst the curves of figure 3.1. Interpolation is possible since the position of the rising part of these curves (the important part for raindrop sizes at these wavelengths) was found to depend mostly on the real part of the refractive index. The values for attenuation by rain at OC obtained in this way were compared with those at 18C and plotted as a correction curve in figure 4.4; the temperature correction curve of Ryde (1946, figure 7) is shown for comparison. They indicate a decrease in attenuation in this wavelength region of about 10% as the tem-

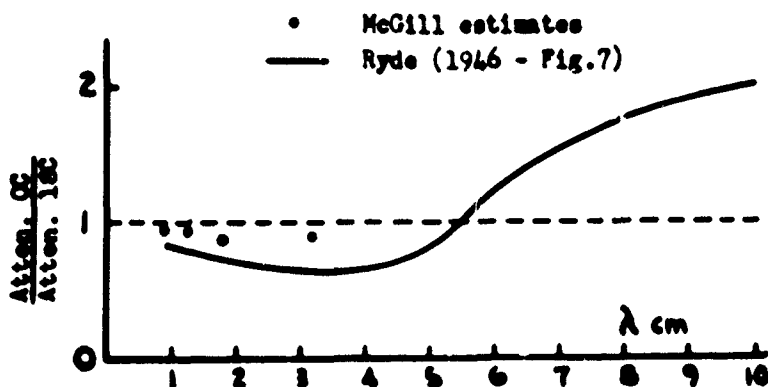


FIG. 4.4 - Approximate temperature correction curve for attenuation by rain (Fig. 7 of Ryde (1946)) with four McGill values superimposed.

perature drops from 19 to 0°C, where Ryde found a 30% decrease. However, since the McGill values are based on an interpolation whose validity could be questioned, it appears that Ryde's (1945) data, from which figure 4.4 was drawn, must be considered the most reliable available.

4.4. Shaped Raindrops

Experiments by Blanchard¹ on water drops in the laboratory suggest that in falling the larger raindrops are flattened into roughly oblate spheroidal shape with axis vertical. Blanchard also shows that when a large drop catches up and collides with a smaller one it will oscillate about an equilibrium shape. Such oscillations can also occur as a result of aerodynamic forces on the drop as it falls. At any time, therefore, a fraction of the total number of drops in the contributing region is non-spherical. Mie's theory does not apply to non-spherical particles, and no complete theory for spheroids is available. An approximate theory for small spheroids which is analogous to the Rayleigh approximations has been used by Atlas, Kerker and Hitschfeld (1953) however, and they find the flattening; diminishes scattering; and attenuation with vertical polarization and enhances it with horizontal polarization. There is not much data available so far on the shape of falling rain.²

This effect cannot account for the difference between measured and predicted average received power because the observations were made with horizontally polarized radars, which would lead to greater measured powers rather than smaller.

1

Blanchard, D.C., 1948: Observations on the behaviour of water drops at terminal velocity in air. General Electric Research Laboratories: Project Cirrus, Occasional Report No. 7.

2

Jones, D.M.A., 1952: Raindrop camera and some preliminary results. Proceedings of the Third Radar Weather Conference, McGill University, page E-9.

5. SNOW

5.1 Scattering by Snow

Dry snow consists of ice particles, either single or aggregated. In the centimetre region, ice has a dielectric constant of 3.17 which is much less than that of water and is independent of wavelength; in the Rayleigh region, scattering is proportional to $|K|^2$ and so the small absorption coefficient K of ice can be neglected. It turns out that the back-scatter cross-section σ for an ice sphere is only about 0.22 times that for a water sphere of the same mass at 3 cm wavelength.

Although an aggregate flake consists of a mixture of air and ice of low mean density, it can be shown (Marshall and Gunn, 1952) that σ is the same as that for the same mass of ice in compact form. Calculations by Atlas, Kerker and Hitschfeld (1953) and by Labrum^{*} indicate that the shape of ice particles or snowflakes is unimportant and that the cross-sections are only slightly greater than those for spheres of the same mass (never more than twice as great). This means that $\sum_1 \sigma$ for snow can be predicted by catching a sample of snowflakes, melting them, measuring $\sum_1 D^6$ for the resulting drops and allowing for the velocity of fall and the dielectric factor.

This was done in Canada by Langille and Thain (1951) who also made radar measurements at the same time. The agreement with the form of equation (1.1) was within the scatter of the observations, but the received power was 4 db less than predicted. As in the rain measurements, this difference is unexplained.

Langille and Thain's results, on further analysis (Marshall and Gunn, 1952) yield an empirical relation between Z and R , where Z refers to unit volume

^{*} Reported by A. J. Higgs: Proc. Third Radar Weather Conf., McGill University, 1952, page F-29.

of snowstorm and is the sum of the sixth powers of the diameters of the flakes when melted, and R is the snowfall rate at the ground measured in millimetres of water per hour. The overall relation is $Z = 200 R^{1.6}$, identical with Canadian results for rain. Since the reflectivity of ice is 0.22 times that of water, radar echoes from snow are 0.22 times those from rain of the same rainfall rate.

5.2 Attenuation by Snow

Attenuation by snow will be partly due to scattering out and partly due to absorption of the incident energy (section 3.2).

According to equations (1.5) and (3.8),

$$\begin{aligned} \text{attenuation (db/km)} &= 0.4343 \sum_1 Q_t \\ &= 0.4343 \left(\sum_1 Q_s + \sum_1 Q_a \right). \end{aligned}$$

We can use the approximate expressions (3.6 and 3.7) if the wavelength is long compared to the particle diameters; the values of $|K|^2$ and $\text{Im}(-K)$ to be used are listed in table 2.2 and are based on Cumming's (1952) values.

This gives

$$\text{attenuation at OC (db/km)} = 0.00349 \frac{R^{1.6}}{\lambda^4} + 0.00224 \frac{R}{\lambda}. \quad (5.1)$$

Ryde (1946) suggests that attenuation by snow in the Rayleigh region and at centimetric wavelengths is given by the second term only. In Table 7.1, values of the attenuation calculated from equation (5.1) for 3 temperatures show that the first term (scattering out) becomes important on going to wavelengths 1 cm and lower. Since Ryde (1946) used refractive index values of Dunsmuir and Lamb (1945) his formula for attenuation by snow must be multiplied by roughly 2 to get the second term in equation (5.1).

5.3 Wet Snow at the "Bright Band"

Atlas, Kerker and Hitschfeld (1953) show that randomly oriented small water spheroids scatter and attenuate more strongly than water spheres of the same volume; the increase is by a factor of 20 or more if the axes of the spheroids are 10 times their diameters.

Labrum^{*} has computed the scattering by an ice ellipsoid coated with water for wavelengths large compared with the size of the particle (corresponding to the Rayleigh approximation for spheres). He finds that even for comparatively thin coatings the composite particle scatters nearly as well as an all-water particle of the same shape. He confirmed this result experimentally.

Extrapolating from the results of Labrum for small water-coated ice spheroids, and Langleben and Gunn^{**} (1952) for larger water-coated spheres and the above-mentioned shape effects for water, it seems not unreasonable to assume that the scattering and attenuation by water-coated ice spheroids of the size of wet snowflakes at radar wavelengths is similar in magnitude to that of spheroidal water drops of the same shape and size.

This can account for the bright band which always appears in radar pictures of steady rain. The bright band is due to a region of enhanced reflectivity a few hundred feet thick just below the 0° isotherm. In the light of the foregoing discussion, the mechanism would be as follows:

Snow falling through the freezing level will change from flat or needle-shaped particles or aggregates which scatter feebly, to similarly-

^{*} loc. cit.

^{**} ibid

shaped particles, which, due to a water coating, scatter relatively strongly. As melting proceeds, they lose their extreme shapes and the shape factor decreases to 1. Also, falling with greater velocity, the number of particles in unit volume becomes less.

Attenuation, like scattering, is proportional to the number of particles per unit volume, and therefore depends on the velocity of fall. Water spheroids absorb more strongly than water spheres, and coated ice spheroids presumably absorb like water spheroids. Therefore, absorption by melting snow will be many times that of the resulting rain. Although the bright band is comparatively thin, serious attenuation may take place when radar observations are made through it at shallow elevations.

6. CLOUDS

Most cloud droplets do not exceed 100 μ diameter, so that at centimetre and millimetre wavelengths the Rayleigh formulae (3.5) (3.6) and (3.7) apply for droplets and equations (1.3) and (1.6) for cloud.

6.1 Scattering from Clouds

Cloud droplets being about one-hundredth the diameter of raindrops, $\sum_1 D^6$ in cloud is about 10^6 less than in rain. However, equation (1.3) for the received power has λ^4 in the denominator, so that it is possible to overcome some of the effect of the very small diameters by going to the shortest practicable wavelength. Radar sets working on wavelengths of 1.25 cm and around 9 mm are now being used for cloud observations.[†] By directing the

[†] See "Proceedings of the Third Radar Weather Conference", McGill University, Montreal, session B.

antenna vertically, the range r_0 is made a minimum, and most clouds visible to the eye are detected by the receiver.

Radar measures the quantity $Z = \sum_1 D^6$, whereas a more significant quantity meteorologically is the liquid water content $M = \frac{\pi}{6} \rho \sum_1 D^3$. To relate the two quantities exactly would require the complete drop size distribution. However, Atlas and Boucher^{*}, after studying a number of such distributions actually observed in clouds, report that a knowledge of the median diameter only is sufficient for a fairly accurate relationship, since the shape of the distribution is similar for all clouds. Even without this knowledge, an approximate correlation between Z and M can be obtained because the median diameter shows a definite trend with M , and this can be incorporated in the empirical law

$$Z = 0.0292 M^{1.82},$$

where M is in gm m^{-3} , and Z in $\text{mm}^6 \text{m}^{-3}$.

6.2 Attenuation by Clouds

Since the cloud particles lie well within the Rayleigh region at all wavelengths in the centimetre band, equation (1.6) applies. The liquid water content $M = \frac{\pi}{6} \sum_1 D^3$, and equation (1.6) becomes

$$\text{attenuation (db/km)} = 0.4343 \frac{6\pi}{\lambda} M \text{Im}(-K)$$

for one-way transmission. Thus attenuation by cloud is dependent on the liquid water content and is independent of the particle size-distribution.

Values of the attenuation from water and ice clouds are given in Table 7.1 as a function of M for four wavelengths and three temperatures. For ice clouds as well as water clouds, $Q_s \ll Q_a$.

^{*} loc. cit. pages B 1-8.

7. THE ATMOSPHERE

7.1 Scattering

Booker and Gordon (1950) have shown that a turbulent atmosphere scatters radio waves in a manner depending on the scale of the turbulence, which may vary from a few cm to a few metres. In particular, long-range point-to-point transmission at centimetre wavelengths can take place by such scattering. In a typical point-to-point case, however, Gordon^{*} has shown that rain will contribute more signal than the turbulence below about 1 metre wavelength and cloud below about 3 cm, provided they fill the space common to the transmitting and receiving beams. Attenuation by the same rain or cloud throughout the path may however reduce the signal below that for clear turbulent air.

Booker and Gordon's equation (2v) gives scattered power in any direction. It depends on the scale of turbulence ℓ which can be thought of as the diameter of the "blobs" of inhomogeneity in the turbulent atmosphere. Making the approximation $4\pi\ell/\lambda \gg 1$, substituting the appropriate angle of scattering and bringing the definition of $\sum_1 \nabla$ into line with section 1 of the present paper, we obtain

$$\sum_1 \nabla = \frac{\overline{(\Delta n)^2}}{2\ell} \times 10^{-6} \text{ cm}^2 \text{ m}^{-3},$$

where $\overline{(\Delta n)^2}$ is the mean square deviation of refractive index in parts per million

and ℓ is the scale in cm.

^{*} Gordon, W. E., 1952: A comparison of radio scattering by precipitation and by a turbulent atmosphere. Proceedings of the Third Radar Weather Conference, McGill University, page F-17.

7.2 Atmospheric Attenuation

Van Vleck (1947) has discussed in detail the mechanism of attenuation in the clear atmosphere.

It has been shown by infrared spectroscopy that oxygen molecules have a magnetic dipole moment, and water vapour molecules have an electric dipole moment. These give rise to lines in their absorption spectra which lie in the centimetre and millimetre region. This means that radio or radar propagation is subject to absorption by the oxygen and water vapour in the atmosphere.

These absorption lines are subject to the usual amount of "pressure broadening". In water vapour, under atmospheric conditions, the most important line has a line half-width of about 0.1 cm^{-1} . Since the wave-number of the line itself is only 0.74 cm^{-1} , however, the line is relatively very broad, having a resonant wavelength of 1.348 cm with half-width of about 0.18 cm , so that its influence extends over much of the microwave region. Additional effects are found due to other absorption lines in the neighborhood of 0.2 cm wavelength.

Becker and Autler (1946) measured the damping of a large cavity resonator filled with air and water vapour. They used wavelengths between 0.75 cm and 1.7 cm . Their results are plotted as part of curve (c) in figure 7.1. The experiments were performed at 450°C , but have been corrected to 200°C in plotting the curve to bring it into line with the other curves. The dashed portions of curve (c) are calculations by Van Vleck from a theoretical formula with the constants chosen to fit Becker and Autler's results. Curve (c) is drawn for 0.001 gm m^{-3} , and attenuation is approximately proportional to water vapour content in the amounts encountered in the atmosphere.

Dicke, Beringer, Kyhl : d Vane (1946) used a radiometer to investigate absorption by atmospheric water vapour at 1.0 cm, 1.25 cm and 1.5 cm. Though the accuracy is not high, the results are consistent with those of Becker and Autler.

The situation for oxygen differs in two respects from that for water vapour; the most important absorption is caused by a number of closely-spaced lines instead of a single line, and, in addition, oxygen has a line at zero frequency, while water vapour has not.

Van Vleck (1947a) predicted the positions of about 25 oxygen absorption lines between 0.45 and 0.56 cm, and these have been measured with a sensitive microwave spectrometer at very low pressures by Barkhalter, Anderson, Smith and Gordy (1950). At atmospheric pressure, however, pressure broadening converts them into an unresolved band of absorption. Lamont (1948) measured attenuation in air from 0.45 to 0.58 cm wavelength over a path of a few km in the field, and his results are plotted as points in figure 7.1.

At the time that Van Vleck's calculations were made, it was believed that the line breadth constant $\Delta\nu$ was the same from line to line, though its value was not known. Accordingly, he assigned several alternative values to $\Delta\nu$ and the predicted attenuation for $\Delta\nu = 0.02 \text{ cm}^{-1}$ and $\Delta\nu = 0.05 \text{ cm}^{-1}$ are plotted against wavelength in figure 7.1, curves (a) and (b). (These are similar to Ryde's (1946) figure 1, curves (a) and (b).)

Van Vleck's predictions include a line at zero frequency, and this accounts for most of the attenuation at wavelengths from 1 cm upwards.^{*} Its intensity is directly proportional to the line breadth and therefore to the pressure, but

^{*} An alternative approach to this kind of absorption can be made by using Debye's theory of polar molecules in dielectrics.

no measurements appear to have been made to determine the line breadth constant. One method is to plot the theoretical curves, choose the one which fits the measured values of attenuation in the 0.5 cm region, and assume the remainder of the curve is also valid. This makes $\Delta\nu = 0.02 \text{ cm}^{-1}$ the best choice (curve (a) of figure 7.1) because it fits Lamont's results the best.

Recent measurements on pure oxygen, however, (see Anderson, Smith and Gordy, 1952) show that the line breadth constant varies from one line to another in the 0.5 cm region; its value lies between 0.03 and 0.05. We cannot say which, if any, of these values applies to the zero-frequency line, so the whole attenuation curve for dry air from 1 cm wavelength upward is unknown. No measurement has been made above 0.6 cm specifically to define the curve, though a single reliable measurement at a wavelength between 1 and 10 cm would suffice.

The possibility remains of using the results of the water vapour experiments already mentioned, by extrapolating to zero water vapour content. Because of their particular experimental method, Becker and Autler found it necessary to eliminate the contribution of oxygen to the absorption in such a way that it cannot be determined. The Radiometer method of Dicke et al (1946) measured combined attenuation of oxygen and various amounts of water vapour, so that if the scatter of the observations were small enough the part due to oxygen could be found by extrapolating to zero water vapour. Only the results at 1.0 cm wavelength are good enough for this; they indicate a most probable value which lies on curve (a) (corresponding to $\Delta\nu = 0.02 \text{ cm}^{-1}$) and that the attenuation is unlikely to be as great as shown by curve (b) which can be taken as an upper limit.

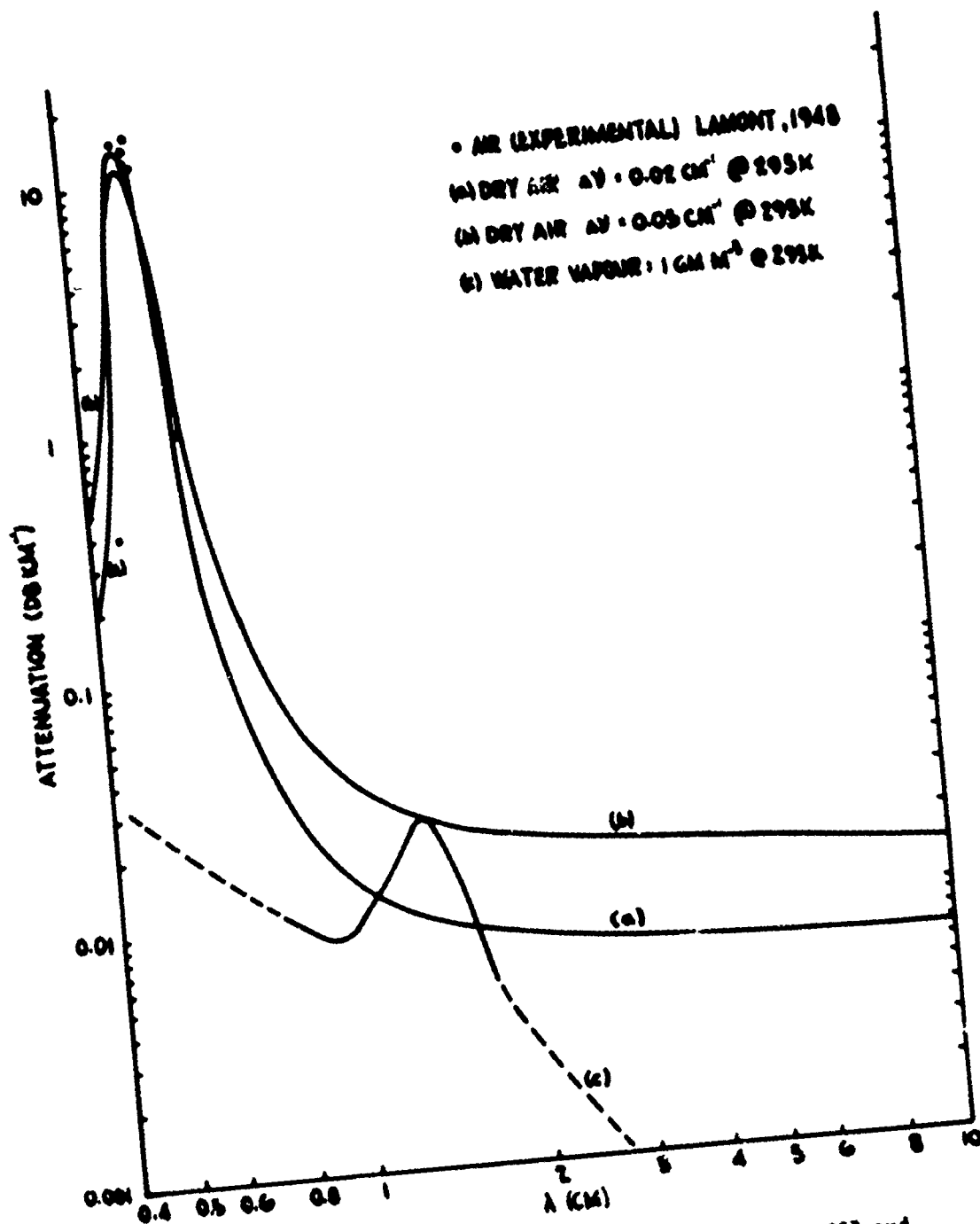


FIG. 7.1 - Attenuation by air and water vapour at 20°C and atmospheric pressure.

Temperatur and pressure are discussed by Van Vleck in his two papers. For a given quantity of water vapour, attenuation is proportional to p^{-1} and to $T^{-2} 10^{-278/T}$ at the maximum of the resonance curve, to p and to $T^{-3} 10^{-278/T}$ on the sides of the curves, and to p and to $T^{-3/2}$ well away from the resonance. Of course, if the air is kept saturated with water vapour while the temperature changes, the water vapour content itself will alter, and this additional factor must be taken into account.

Pressure effect on atmospheric oxygen arises from increased pressure broadening and also from an increase in the number of molecules per unit volume. In the region of strong absorption, the attenuation is proportional to p and to $T^{-3/2}$, but in the region of the "zero-frequency" absorption (from say 2 to 10 cm wavelength) it is proportional to p^2 and to $T^{-5/2}$.

Table 7.1 is a summary of the results of the preceding sections and gives working values of the attenuation by rain, snow and clouds.

T. NLE 7.1

Working Values of ATTENUATION in db.km^{-1} (one way)

	Temp (C)	λ	3.2 cm	1.8 cm	1.24 cm	0.9 cm
		10^{22}				
RAIN ^a R in mm.hr^{-1}			$0.0074R^{1.31}$	$0.045R^{1.14}$	$0.12R^{1.05}$	$0.22R^{1.00}$
SNOW ^b R in mm.hr^{-1} of melted water	0		$3.3 \times 10^{-5} R^{1.6}$ + $68.6 \times 10^{-5} R$	$3.32 \times 10^{-4} R^{1.6}$ + $12.2 \times 10^{-4} R$	$1.48 \times 10^{-3} R^{1.6}$ + $1.79 \times 10^{-3} R$	$5.39 \times 10^{-3} R^{1.6}$ + $2.44 \times 10^{-3} R$
	-10		$3.3 \times 10^{-5} R^{1.6}$ + $22.9 \times 10^{-5} R$	$3.32 \times 10^{-4} R^{1.6}$ + $4.06 \times 10^{-4} R$	$1.48 \times 10^{-3} R^{1.6}$ + $0.59 \times 10^{-3} R$	$5.39 \times 10^{-3} R^{1.6}$ + $0.81 \times 10^{-3} R$
	-20		$3.3 \times 10^{-5} R^{1.6}$ + $15.7 \times 10^{-5} R$	$3.32 \times 10^{-4} R^{1.6}$ + $2.80 \times 10^{-4} R$	$1.48 \times 10^{-3} R^{1.6}$ + $0.41 \times 10^{-3} R$	$5.3 \times 10^{-3} R^{1.6}$ + $0.56 \times 10^{-3} R$
WATER CLOUD M in gm.m^{-3}	20		0.0483 M	0.128 M	0.311 M	0.647 M
	10		0.0630 M	0.179 M	0.406 M	0.681 M
	0		0.0859 M	0.267 M	0.532 M	0.99 M
	-8		0.112 M (extrapolated)		0.684 M	
ICE CLOUD M in gm.m^{-3}	0		$2.46 \times 10^{-3} M$	$4.36 \times 10^{-3} M$	$6.35 \times 10^{-3} M$	$8.74 \times 10^{-3} M$
	-10		$8.19 \times 10^{-4} M$	$1.46 \times 10^{-3} M$	$2.11 \times 10^{-3} M$	$2.91 \times 10^{-3} M$
	-20		$5.63 \times 10^{-4} M$	$1 \times 10^{-3} M$	$1.45 \times 10^{-3} M$	$2 \times 10^{-3} M$

* These are empirical equations. For the more exact relations on which they are based, see section 4.3 and figure 4.3.

** The effect of temperature is discussed in section 4.3 and summarized in figure 4.4. The effect of non-sphericity on Q_{ext} and Q_{scat} has been neglected.

* As long as snowflakes are in the Rayleigh region. A value of $R=10$ or $R^{1.6}=99$ is an upper limit for snowfall rates.

8. THE DIRECTION OF FUTURE RESEARCH

8.1 Refractive Indices

The measured values of the refractive index of water for various wavelengths and temperatures are quite adequate for microwave-precipitation work. The fact that the measured values fit the theoretical formulae so well (see, for example Saxton, 1946) allows interpolation and extrapolation about these values to be made with confidence.

The situation for ice is not so well established. There is agreement on the value of the real part of the refractive index and on its independence of temperature and wavelength variation in the microwave region. However, measured values of the imaginary part differ by a factor 2. Probably further determinations of this quantity are in order.

8.2 Rain

While anomalies in raindrop size-distributions continue to be reported, they seem to appear at an equilibrium rate and make a very small dilution of the general broadagreement. Data will continue to accumulate as an adjunct of any scattering and attenuation measurements that are made. For a better understanding of the rain mechanism, a more detailed study of the size-distribution with time from a given shower, and variations with precipitation type, is needed.

Though Ryde (1945) evaluated the attenuation by rain at four wavelengths, and various temperatures, the work may bear repeating for the slightly changed values of the refractive index of water which have been reported since his computations were made. The final results

should not be very different but in view of the appreciable attenuation by rain, and the magnitude of the computational work, it might be worth while essentially repeating Ryde's work by compiling a table of the Mie amplitude functions for water at OC similar to Lowan's (1949) 18C table.

If non-spherical drops occur in natural rain, the scattering and attenuation could be considerably affected. Shaped raindrops are thought to be rare but a raindrop photography program undertaken recently by the Illinois State Water Survey should provide a definite answer to this problem.

There is a general scarcity of point to point measurements of attenuation by rain.

One outstanding unsolved problem is the source of the 4-7 db. difference between the actual signal received from both rain and snow and that predicted from the theory.

8.3 Snow

The dielectric properties of ice and snow and wet snow have been measured in the lab by Cumming (1952). There is still, however, the disagreement about the value of the imaginary part (k) of the refractive index. Labrum in Australia has observed the scattering from single melting spheroidal ice particles.

There has been little experimental work done on either scattering or attenuation by falling snow. There is a need for laboratory experiments to study the melting of natural snowflakes, both single crystals and aggregates. Point to point measurements of attenuation by melting snow would be particularly valuable.

8.4 Cloud

Laboratory experiments on the scattering by single water spheres have been done, and give results in good agreement with theory. Laboratory experiments to determine the dielectric properties of water cloud are possible and might provide amongst other things a possible clue to the 4-7 db discrepancy between actual and predicted scattering mentioned above.

8.5 Atmosphere

The attenuation due to water vapour has only been measured at wavelengths 0.7 and 1.7 cm, but the necessary theoretical basis for extrapolating beyond these limits seems to be satisfactory.

The most noticeable gap in present knowledge of atmospheric attenuation is a direct and reliable measurement of the zero-frequency line in oxygen under atmospheric conditions.

A laboratory experiment at any wavelength over 1 cm on dry air at atmospheric and at very low pressures, or a field experiment at any wavelength over 3 cm at a low humidity would determine the line breadth constant and remove the uncertainty at all wavelengths above the 0.5 cm band. However, since the attenuation appears to be not much greater than 0.01 db/km it is difficult to measure and at the same time usually unimportant in practice. Any application in which it becomes important to know it precisely will probably suggest a way of measuring it accurately.